

Anomalous kinetic properties of metals near the Lifshitz topological transition

A. A. Varlamov and A. V. Pantsulaya

Moscow Institute of Steel and Alloys

(Submitted 13 June 1985)

Zh. Eksp. Teor. Fiz. **89**, 2188–2196 (December 1985)

The behavior of the conductivity and thermoelectric power in the vicinity of a point at which the topology of the Fermi surface of a metal change is investigated at finite temperature and impurity density. It is shown that the previously predicted thermoelectric-power singularity near the topological transition is eliminated when account is taken of these two factors. The laws governing the variation of the conductivity and of the thermoelectric power, as well as their temperature dependences, are determined on the right and left of the transition point. The results explain the available experimental data.

1. Interest in the study of the electronic topological transitions predicted by Lifshitz,¹ in various metals and alloys, has increased noticeably of late.^{2–9} Investigation of the thermodynamic, and especially kinetic, properties of substances undergoing such transitions not only confirms the very existence of the transition in the system, but yields information on various electronic properties (such as the relaxation times of small carrier groups).

It is pointed out even in I. M. Lifshitz's trail-blazing paper¹ that when the topology of the Fermi surface of a metal is changed, the thermodynamic quantities, and also the kinetic coefficients should have on one of the sides of such a transition singularities of the type $|z|^{\pm 1/2}$, where z is a continuously varying parameter that indicates proximity of the system to a phase transition of order $2\ 1/2$ and vanished at the transition point itself.

Vaks *et al.*² have shown that the thermoelectric power has in this case a singularity of type $|z|^{-1/2}$, whereas other kinetic coefficients have a much weaker z -dependence ($\sim |z|^{1/2}$). This conclusion was arrived at by pseudopotential-theory methods with a transition of order $2\ 1/2$ in the $\text{Li}_{1-x}\text{Mg}_x$ alloy as the example. At the same time, Egorov *et al.*³ investigated experimentally the thermoelectric power in these alloys at various Mg concentrations and have indeed observed in the thermoelectric power at $x_c \approx 0.2$ an anomaly that manifested itself distinctly at nitrogen and helium temperatures. In the analysis of the experimental results, however, it was pointed out in Ref. 3 that the observed dependence of the thermoelectric power on z (on the Mg concentration in that particular case, $z = x - x_c$) differed substantially from the that predicted in Ref. 2. In place of the divergence as $z \rightarrow -0$ and the jump of the thermoelectric power to its normal value at $z > 0$ (Ref. 2), the experiment of Ref. 3 showed a rather broad peak with a smooth fall to the normal value of the thermoelectric power in the $z > 0$ region. It was proposed in Ref. 3 that allowance for electron scattering by impurities can lead to a finite thermoelectric power at the peak and make the latter more symmetric than predicted in Ref. 2.

We investigate in the present paper the behavior of the differential thermoelectric power $Q(z, T)$ on the conductivity $\sigma(z, T)$ in the vicinity of the point where a $2\ 1/2$ phase

transition would take place at $T = 0$ in the absence of impurities. It will be shown that in the presence of impurities and at finite temperatures, when the variation of the Fermi-surface topology is not a $2\ 1/2$ phase transition in its rigorous meaning (we shall refer to this situation as the Lifshitz topological transition), the thermoelectric power has an anomaly as before. However, the divergence at $z = 0$ (Ref. 2) is no longer present and becomes smeared out by the temperature (so long as $T \gtrsim \tau^{-1}$) or by the characteristic relaxation time τ (at $T \lesssim \tau^{-1/2}$). In the pure case ($\tau \gg T - 1$) the peak of $Q(z)$ is strongly asymmetric and as the temperature is raised it decreases, spreads out, and shifts towards larger negative z . In the dirty case ($\tau \leq T^{-1}$) the peak broadens but retains as before some asymmetry, albeit a weaker one than at $\tau \gg T^{-1}$.

The conductivity anomaly in a phase transition of order $2\ 1/2$ is of the kink type.^{1,2} When impurity scattering and the finite temperature are taken into account, the kink is smoothed out, but the characteristic $\sigma(z, T, \tau)$ dependence together with the change of the thermoelectric power can attest to a change of the topology of the Fermi surface.

2. The change of the Fermi-surface topology in real metals and in alloys can take a large variety of forms: formation or breaking of a neck, the onset or vanishing of a cavity, spillover of electrons from several ellipsoids into one, etc.

We shall consider the simple "neck-breaking" transition. In view of the qualitative agreement between our present results with the experimentally measured thermoelectric powers of $n - \text{Bi}_{0.9}\text{Sb}_{0.1}$ compounds,⁴ where electrons spill over from three electron ellipsoids into one, suggests that the choice of a specific type of transition is of no fundamental significance.

To simulate a neck-breaking transition, we choose the Fermi surface to be a hyperboloid of revolution (Fig. 1)

$$\frac{p_{\perp}^2}{2m_{\perp}} - \frac{p_x^2}{2m_x} = \mu - E_c = z, \quad (1)$$

where \mathbf{P}_{\perp} and p_x are the transverse and longitudinal components of the electron momentum, and E_c is a certain critical energy corresponding to the topological transition. External factors (e.g., pressure) change the chemical potential and the single-sheet hyperboloid ($\mu > E_c$) becomes two-sheeted ($\mu < E_c$), and this corresponds in fact to a neck-breaking

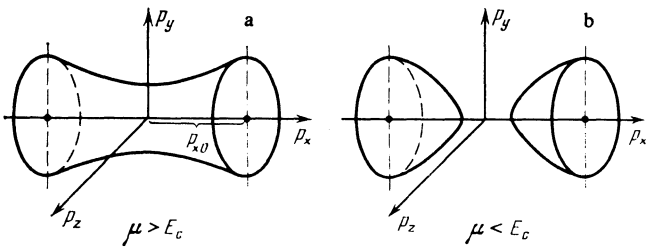


FIG. 1. Topological transition of the "neck-breaking" type. At $z = 0$ the open Fermi surface (a) turns into a closed one (b): p_{x0} is the limiting value of the longitudinal momentum.

topological transition.

To find the kinetic coefficients near such a transition, we use a temperature diagrammatic technique. We must first calculate the one-electron Green's function with anisotropic spectrum (1) and with allowance for scattering by the impurities

$$G^{-1}(\omega_n, \mathbf{p}) = i\omega_n - \frac{\mathbf{p}_\perp^2}{2m_\perp} + \frac{p_x^2}{2m_x} + z - \Sigma(\omega_n, z), \quad (2)$$

where $\omega_n = 2\pi T(n + \frac{1}{2})$.

If the impurity density is not too high ($\varepsilon_0 \tau \gg 1$), where $\varepsilon_0 = P_{x0}^2/2m_x$ is an energy of the order of μ and corresponds to the limiting momentum p_{x0} , while τ is the characteristic relaxation time which we shall define below), the self-energy part Σ can be calculated in the ladder approximation.¹⁰ Assuming for simplicity pointlike and isotropic scattering by the impurities, we can write for Σ the self-consistent equation

$$\Sigma(\omega_n, z) = n_i |u|^2 \int \frac{d^3 p}{(2\pi)^3} \left[i\omega_n - \frac{\mathbf{p}_\perp^2}{2m_\perp} + \frac{p_x^2}{2m_x} + z - \Sigma(\omega_n, z) \right]^{-1}; \quad (3)$$

here n_i is the impurity density and $|u|$ is the amplitude of the electron scattering by the impurities and is assumed constant.

Analytic continuation of $\Sigma(\omega_n, z)$ into the upper complex-frequency half-plane (via the substitution $i\omega_n \rightarrow \omega$) and integration over the momenta, followed by separation of the real and imaginary parts of the resultant equation, yields

$$\text{Im } \Sigma^R(\omega, z) = -\frac{1}{2V2\tau} \left\{ \left[\left(1 + \frac{\text{Re } \Sigma^R}{\varepsilon_0} - \frac{\omega}{\varepsilon_0} \right)^2 + \frac{\text{Im}^2 \Sigma^R}{\varepsilon_0^2} \right]^{1/2} + 1 + \frac{\text{Re } \Sigma^R}{\varepsilon_0} - \frac{\omega}{\varepsilon_0} \right\}^{1/2} - \left[\left(\frac{\text{Re } \Sigma^R}{\varepsilon_0} - \frac{\omega}{\varepsilon_0} - \frac{z}{\varepsilon_0} \right)^2 + \frac{\text{Im}^2 \Sigma^R}{\varepsilon_0^2} \right]^{1/2} + \frac{\text{Re } \Sigma^R}{\varepsilon_0} - \frac{\omega}{\varepsilon_0} - \frac{z}{\varepsilon_0} \right]^{1/2}, \quad (4)$$

$$\text{Re } \Sigma^R(\omega, z) = -\frac{1}{2V2\tau} \left\{ \left[\left(1 + \frac{\text{Re } \Sigma^R}{\varepsilon_0} - \frac{\omega}{\varepsilon_0} \right)^2 + \frac{\text{Im}^2 \Sigma^R}{\varepsilon_0^2} \right]^{1/2} - 1 - \frac{\text{Re } \Sigma^R}{\varepsilon_0} + \frac{\omega}{\varepsilon_0} \right\}^{1/2} - \left[\left(\frac{\text{Re } \Sigma^R}{\varepsilon_0} - \frac{\omega}{\varepsilon_0} - \frac{z}{\varepsilon_0} \right)^2 + \frac{\text{Im}^2 \Sigma^R}{\varepsilon_0^2} \right]^{1/2} - \frac{\text{Re } \Sigma^R}{\varepsilon_0} + \frac{\omega}{\varepsilon_0} + \frac{z}{\varepsilon_0} \right]^{1/2}.$$

We have introduced here the characteristic relaxation time

$$\tau^{-1} = \pi^{-1} n_i |u|^2 m_\perp (2m_x \varepsilon_0)^{1/2}. \quad (5)$$

It can be seen from the system (4) that the real part $\text{Re } \Sigma^R$ is small in terms of $(\varepsilon_0 \tau)^{-1}$ compared with $\text{Im } \Sigma^R$, and the corresponding contribution to the Green's function can be neglected.

In the pure case ($T \gg \tau^{-1}$) the relation $\text{Im } \Sigma^R \ll T$ is valid. The essential frequency region for the subsequent integrations is $|\omega| \lesssim T$, so that small terms of the type $\text{Im}^2 \Sigma^R / \varepsilon_0^2$ can be neglected in (4), and we obtain

$$\text{Im } \Sigma^R(\omega, z) = -\frac{1}{2\tau} \left\{ \left(1 - \frac{\omega}{\varepsilon_0} \right)^{1/2} \theta(\varepsilon_0 - \omega) - \left(\frac{|z + \omega|}{\varepsilon_0} \right)^{1/2} \theta(-(z + \omega)) \right\}, \quad (6)$$

where $\theta(x)$ is the Heaviside theta function.

In the opposite ("dirty") case ($T \ll \tau^{-1}$) the system (4) can be solved by successive approximations with respect to the parameter $(\varepsilon_0 \tau)^{-1}$. The result is

$$\text{Im } \Sigma^R(\omega, z) = -\frac{1}{2\tau} \left\{ 1 - \frac{\omega}{2\varepsilon_0} - \frac{1}{\sqrt{2}} \left[\left[\frac{1}{4\tau^2 \varepsilon_0^2} + \frac{(\omega + z)^2}{\varepsilon_0^2} \right]^{1/2} - \frac{\omega + z}{\varepsilon_0} \right]^{1/2} \right\}. \quad (7)$$

3. The kinetic coefficients can be expressed in terms of the correlators of the one-electron temperature Green's functions.¹¹ For the conductivity σ_{ik} this correlator reduces to the usual electromagnetic-response operator, whose vertex functions $\gamma_i^{(e)} = e \partial \varepsilon(p) / \partial p_i = ev_i$ correspond to interaction of an electron with an electromagnetic field (Fig. 2), where the function $\varepsilon(p)$ determines the conduction-electrons dispersion law.

The off-diagonal kinetic coefficients β_{ik} in the expression $Q_{ik} = -\sigma_{in}^{-1} \beta_{nk}$ for the differential thermoelectric power is determined graphically by an identical diagram, but one of its vertices corresponds to the heat-flux operator. In the case of interest to us of not too high temperatures, the electron-phonon and interelectron interactions can be neglected, and the vertex corresponding to the heat flux takes in the (\mathbf{p}, ω_n) representation the form $\gamma_j^{(h)} = i\omega_n v_j$, where ω_n is the fermion frequency that runs over the electron lines. The averaging of the corresponding diagrams over the impurity positions is standard¹⁰ and reduces to averaging the Green's functions themselves (renormalization of the vector vertex in case of anisotropic scattering would lead only to the substitution $\tau \rightarrow \tau_{tr}$) an averaging already carried out above. Thus, the correlators $K_{ij}^{(ee)}(\Omega_\nu)$ and $K_{ij}^{(eh)}(\Omega_\nu)$ are represented in the form

$$\begin{pmatrix} K_{ij}^{(ee)} \\ K_{ij}^{(eh)} \end{pmatrix} = 2T \sum_{\omega_n} \int \frac{d^3 p}{(2\pi)^3} \gamma_i^{(e)} \begin{pmatrix} \gamma_j^{(e)} \\ \frac{1}{2} \gamma_j^{(h)} \end{pmatrix} G(\omega_n + \Omega_\nu, \mathbf{p}) G(\omega_n, \mathbf{p}), \quad (8)$$

where Ω_ν is the external Boson frequency. Transforming the sums over the frequencies into contour integrals and contin-

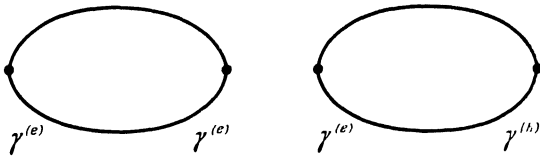


FIG. 2.

using analytically in the usual manner ($i\Omega_v \rightarrow \Omega$) the frequency correlators into the upper complex-frequency half-plane, we obtain for the kinetic coefficients

$$\left(\begin{array}{c} \sigma_{xx} \\ \beta_{xx} \end{array} \right) = \frac{em_{\perp}}{48\pi^2 m_x^{1/2} T^2} \int_{-\infty}^{\infty} \frac{d\omega}{\text{ch}^2(\omega/2T)} \left(\frac{2eT}{\omega} \right) \frac{[(\varepsilon_0 - \omega)^2 + \text{Im}^2 \Sigma^R]^{1/2} + \varepsilon_0 - \omega}{|\text{Im} \Sigma^R(\omega)|} \frac{d\omega}{\text{ch}^2(\omega/2T)} \text{Im}^2 G^R(\omega, \mathbf{p}, z). \quad (10)$$

This expression, in conjunction with the self-energy part $\Sigma^R(\omega, z)$ obtained above, determines in general form the thermoelectric power and the conductivity of a metal near a $2\frac{1}{2}$ -order phase transition of the neck-breaking type at $T \neq 0$ and in the presence of electron scattering by impurities.

4. We consider first the case of a pure metal ($T \gg \tau^{-1}$). We can then neglect in (10) the quantity $\text{Im}^2 \Sigma^R$ in the radicands, since the main contribution in integration with respect to ω is made by the frequency region $|\omega| \leq T$. using expression (6) $\text{Im} \varepsilon^R$, we get

$$\left(\begin{array}{c} \sigma_{xx} \\ \beta_{xx} \end{array} \right) = \frac{em_{\perp} \tau (2\varepsilon_0)^{1/2}}{12\pi^2 m_x^{1/2} T^2} \int_{-\infty}^{\infty} \left(\frac{2eT}{\omega} \right) \frac{d\omega}{\text{ch}^2(\omega/2T)} \times \frac{(\varepsilon_0 - \omega)^{1/2} \theta(\varepsilon_0 - \omega) - |\omega + z|^{1/2} \theta(-(\omega + z))}{(\varepsilon_0 - \omega)^{1/2} \theta(\varepsilon_0 - \omega) - |\omega + z|^{1/2} \theta(-(\omega + z))}, \quad (11)$$

whence, after simple calculations, we get

$$\sigma_{xx} = \sigma_0 \begin{cases} 1 + \left(\frac{|z|}{\varepsilon_0} \right)^{1/2} & z \ll -T, \\ 1 + 0.54 \left(\frac{T}{\varepsilon_0} \right)^{1/2} \left(1 - 0.68 \frac{z}{T} \right) & |z| \ll T, \\ 1 + 0.89 \left(\frac{T}{\varepsilon_0} \right)^{1/2} \exp\left(-\frac{z}{T}\right) & z \gg T, \end{cases} \quad (12a, 12b, 12c)$$

$$Q_{xx} = Q_0 \begin{cases} 1 + \frac{1}{4} \left(\frac{\varepsilon_0}{|z|} \right)^{1/2} & z \ll -T, \\ 0.14 \left(\frac{\varepsilon_0}{T} \right)^{1/2} \left(1 - 0.29 \frac{z}{T} \right) & |z| \ll T, \\ 0.5 + 0.18 \left(\frac{\varepsilon_0}{T} \right)^{1/2} \frac{z}{T} \exp\left(-\frac{z}{T}\right) & z \gg T, \end{cases} \quad (13a, 13b, 13c)$$

where

$$\sigma_0 = \frac{e^2 m_{\perp} \tau (2\varepsilon_0)^{1/2}}{3\pi^2 m_x^{1/2}}, \quad Q_0 = \frac{\pi^2 T}{3e\varepsilon_0}$$

are the conductivity and differential thermoelectric power of a normal metal far from the transition. It can be seen from (12) that in the pure case the conductivity anomaly at $T = 0$ is kink-shaped, as before, in accord with the results of Refs. 1 and 2. At finite temperature, the kink smoothes out and in the region $|z| \leq T$ the conductivity varies smoothly near the transition point. A schematic plot of the conductivity versus

$$\left(\begin{array}{c} \sigma_{ij} \\ \beta_{ij} \end{array} \right) = \lim_{\Omega \rightarrow 0} \frac{1}{-i\Omega T} \left(\begin{array}{c} [K_{ij}^{(ee)}]^{RT} \\ [K_{ij}^{(eh)}]^{RT} \end{array} \right) = \frac{e}{4\pi T^2} \int v_i v_j \frac{d^3 p}{(2\pi)^3} \int_{-\infty}^{\infty} \left(\frac{2eT}{\omega} \right) \frac{d\omega}{\text{ch}^2(\omega/2T)} \text{Im}^2 G^R(\omega, \mathbf{p}, z). \quad (9)$$

Substituting in (9) the explicit expression (1) for $G^R(\omega, \mathbf{p}, z)$ and integrating over the momenta, we obtain for the longitudinal components σ_{xx} and β_{xx}

z is shown in Fig. 3 (curve a).

It follows from (13) that the differential thermoelectric power reaches, accurate to a coefficient that depends on the Fermi-surface geometry, its value Q_0 for an isotropic normal metal. As the transition is approached from the side of negative z (this corresponds to a two-cavity hyperboloid) the thermoelectric power increases in proportion to $|z|^{-1/2}$ and reaches at $z_c = -1.28T$ its maximum value $Q_{\text{max}} \approx 0.19Q_0 \varepsilon_0^{1/2} / T^{1/2}$. The value of z_c is determined by solving numerically the equation

$$\int_0^{\infty} x^{-1/2} (x+z) \text{ch}^{-2} \left(\frac{x+z}{2T} \right) dx = 0.$$

Note that Q_{max} exceeds Q_0 in terms of the large parameter $(\varepsilon_0/T)^{1/2}$ and it can be stated in this sense that a giant thermoelectric power is present in the region of $|z| \lesssim T$. We emphasize once more that the thermoelectric power reaches its maximum not at the transition point itself, but close to it. This can be treated as a result of the "temperature breakdown" that occurs when the Fermi surface approaches the boundary of the Brillouin zone. With further increase of positive z the Fermi surface is transformed into a one-cavity hyperboloid and the thermoelectric power begins to decrease rapidly (exponentially) from its anomalously large value at $z = 0$ to the normal value Q_0 at $z \gtrsim T$. This behavior

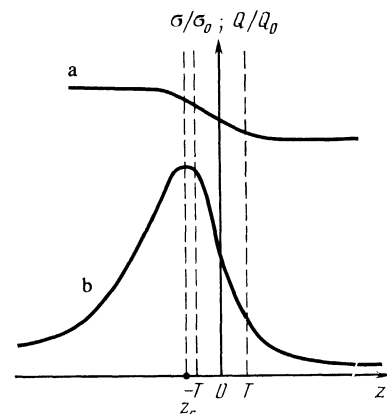


FIG. 3. Schematic plots of the conductivity (curve a) and of the differential thermoelectric power (curve b) versus the parameter z (pure case).

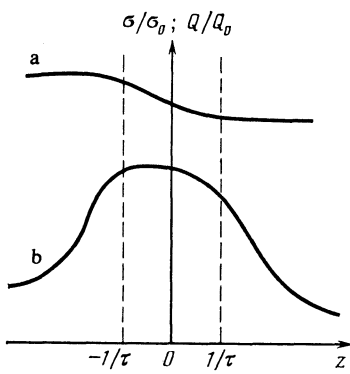


FIG. 4. Schematic plot of the conductivity (curve *a*) and of the differential thermoelectric power (curve *b*) versus the parameter *z* (dirty case).

is illustrated schematically in Fig. 3 (curve *b*).

5. We consider now a dirty metal ($T \lesssim \tau^{-1} \ll \varepsilon_0$). We can no longer neglect $\text{Im}^2 \Sigma^R$ in the radicands of (10). The characteristic parameter with which z should be compared is now not the temperature but τ^{-1} . In the vicinity of the transition, where $|z| \ll \tau^{-1}$ expression (7) can be simplified by expanding in the small parameter $z\tau(\varepsilon_0\tau)^{1/2}$. This yields

$$\text{Im} \Sigma^R = -\frac{1}{2\tau} \left(1 - \frac{1}{2(\varepsilon_0\tau)^{1/2}} \right) - \frac{\omega+z}{4} \frac{1}{(\varepsilon_0\tau)^{1/2}}. \quad (14)$$

In the case of large negative z ($z \lesssim -\tau^{-1}$) we can neglect τ^{-1} compared with z in expression (7) for the self-energy part. Even though $\tau^{-1} \gg T$, the situation turns out to be similar to that in the pure case. Expressions (12a) and (13a) remain therefore valid for the conductivity and for the thermoelectric power respectively in the region $z \lesssim -\tau^{-1}$.

Nothing like that occurs, however, at large positive z ($z \gtrsim \tau^{-1}$), and the picture is substantially different from that in the corresponding region ($z \gtrsim T$) in the pure case. Expanding the radicands in (7) we see that the terms $(\omega+z)/2$ cancel out also in the region $\tau^{-1} \lesssim z \lesssim \tau^{-1}(\varepsilon_0\tau)^{1/3}$; for the self-energy part we get

$$\text{Im} \Sigma^R = -\frac{1}{2\tau} \left[1 - \frac{1}{4\tau(\varepsilon_0z)^{1/2}} \left(1 - \frac{\omega}{2z} \right) \right]. \quad (15)$$

It is now easy to obtain explicit expressions for the conductivity and the differential thermoelectric power in the dirty case. Substituting expressions (14) and (15) for $\text{Im} \Sigma^R$ in (10) and calculating the remaining integral with respect to frequency, we get

$$\sigma_{xx} = \sigma_0 \begin{cases} 1 + (|z|/\varepsilon_0)^{1/2} & z \lesssim -\tau^{-1}, \\ 1 + 1/2(\varepsilon_0\tau)^{-1/2}(1-z\tau) & |z| \ll \tau^{-1}, \\ 1 + 1/2\tau^{-1}(\varepsilon_0z)^{-1/2} & \tau^{-1} \lesssim z \lesssim \tau^{-1}(\varepsilon_0\tau)^{1/3}, \end{cases} \quad (16a)$$

$$\sigma_{xx} = \sigma_0 \begin{cases} 1 + 1/2(\varepsilon_0\tau)^{-1/2}(1-z\tau) & |z| \ll \tau^{-1}, \\ 1 + 1/2\tau^{-1}(\varepsilon_0z)^{-1/2} & \tau^{-1} \lesssim z \lesssim \tau^{-1}(\varepsilon_0\tau)^{1/3}, \end{cases} \quad (16b)$$

$$\sigma_{xx} = \sigma_0 \begin{cases} 1 + 1/4(\varepsilon_0/|z|)^{1/2} & z \lesssim -\tau^{-1}, \\ 1 + 1/4(\varepsilon_0\tau)^{1/2}(1-1.5z/\varepsilon_0) & |z| \ll \tau^{-1}, \\ 3/4 + 0.06\varepsilon_0^{1/2}/\tau z^{1/2} & \tau^{-1} \lesssim z \lesssim \tau^{-1}(\varepsilon_0\tau)^{1/3}. \end{cases} \quad (17a)$$

$$Q_{xx} = Q_0 \begin{cases} 1 + 1/4(\varepsilon_0/|z|)^{1/2} & z \lesssim -\tau^{-1}, \\ 1 + 1/4(\varepsilon_0\tau)^{1/2}(1-1.5z/\varepsilon_0) & |z| \ll \tau^{-1}, \\ 3/4 + 0.06\varepsilon_0^{1/2}/\tau z^{1/2} & \tau^{-1} \lesssim z \lesssim \tau^{-1}(\varepsilon_0\tau)^{1/3}. \end{cases} \quad (17b)$$

$$Q_{xx} = Q_0 \begin{cases} 1 + 1/4(\varepsilon_0/|z|)^{1/2} & z \lesssim -\tau^{-1}, \\ 1 + 1/4(\varepsilon_0\tau)^{1/2}(1-1.5z/\varepsilon_0) & |z| \ll \tau^{-1}, \\ 3/4 + 0.06\varepsilon_0^{1/2}/\tau z^{1/2} & \tau^{-1} \lesssim z \lesssim \tau^{-1}(\varepsilon_0\tau)^{1/3}. \end{cases} \quad (17c)$$

We see from (16) that the conductivity kink^{1,2} for a topological transition in the presence of impurities is smoothed out by impurity scattering of the electrons even at $T=0$. The kink is now smeared out in the wider (compared with temperature region $|z| \lesssim \tau^{-1}$). A schematic plot of the conductivity versus the parameter z is shown by curve *a* of Fig. 4.

The differential thermoelectric power in a dirty metal near a topological transition is described by expressions (17). It can be seen that in this case an anomaly appears, as before, near the transition, but it is now less pronounced: $Q_{\text{max}}/Q_0 \sim (\varepsilon_0\tau)^{1/2}$ in place of $Q_{\text{max}}/Q_0 \sim (\varepsilon_0/T)^{1/2}$. A schematic plot of $Q(z)$ in the dirty case is shown in Fig. 4, curve *b*. As z increases from large negative values to τ^{-1} , the thermoelectric power exhibits the usual square-root growth ($\propto |z|^{-1/2}$) from the value $2Q_0$ to $Q_{\text{max}} \approx (\varepsilon_0\tau)^{1/2}Q_0$ at $z \sim -\tau^{-1}$, after which the growth slows down rapidly and the plot practically flattens out (a weakly pronounced maximum appears at $z \sim \tau^{-1}$). With further increase of z ($\tau^{-1} \lesssim z \lesssim \tau^{-1}(\varepsilon_0\tau)^{1/3}$) the thermoelectric power begins to decrease like $z^{-3/2}$ and consequently the asymmetry of the peak is preserved also in the dirty case. Recall that in the pure case to the right of the peak ($z \gtrsim T$) the thermoelectric power decreased rapidly (exponentially) to its normal value. In the considered case $\tau^{-1} \gg T$, however, the impurities lead, as assumed in the analysis of the experiments,³ both to a broadening of the peak and to a smoother decrease (power-law rather than exponential) of the thermoelectric power on the right of the transition. We point out also that the impurity not only eliminate the formal divergence at the point $z=0$ (at $T=0$) (Ref. 2), but also limit the maximum possible value of the thermoelectric power at small finite temperatures ($T\tau \ll 1$) in terms of the parameter $(T\tau)^{1/2}$, thereby smoothing the peak even more. In the region $z > \tau^{-1}(\varepsilon_0\tau)^{1/3}$, the thermoelectric power is of its normal order of magnitude, and we shall not present the corresponding expression.

6. To conclude, we discuss the obtained functions $Q(z, T)$ and $\sigma(z, T)$ and analyze the available experimental results.

At high temperatures, the condition $T\tau \gg 1$ is satisfied for a sufficiently pure metal. Therefore, according to (13), as the temperature is lowered ($\tau^{-1} \lesssim T \ll \varepsilon_0$) a peak of the function $Q(z, T)/Q_0(T)$ evolves near the topological transition (Fig. 5) and increases like $(|\varepsilon_0|/T)^{1/2}$. With further lowering of the temperature, when T becomes of the order of τ^{-1} , the dependence of $Q(z)/Q_0$ on temperature vanishes [see (17)] and the final shape of the curve is determined by the characteristic relaxation time τ .

As before, however, $Q(z)/Q_0$ has a square-root growth up to $z \approx \tau^{-1}$ in the large-connectivity region ($z < 0$). It is

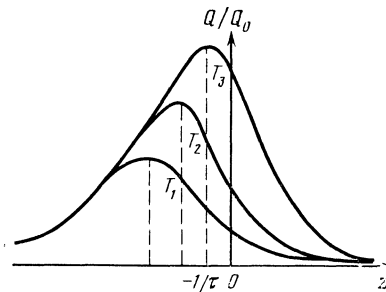


FIG. 5. Reduced differential thermoelectric power vs the parameter z at various temperatures ($T_1 > T_2 > \tau^{-1}$, $T_3 < \tau^{-1}$). At $T \lesssim \tau^{-1}$ the reduced differential thermoelectric power ceases to depend on temperature.

replaced next, in the region $|z| \lesssim \tau^{-1}$, by a plateau (inclusion, in the vicinity of $z = 0$, of the next terms of the expansion in the parameter z/ε_0 in (17) shows that traces of the maximum, which was reached at $z_c = -1.28T$ in the pure case, still remain near the point $z \approx -\tau^{-1}$). The exponential decrease on the right of the transition at high temperatures for $z \gtrsim T$ gives way now to a power-law decrease like $z^{-3/2}$ (at $z \gtrsim \tau^{-1}$).

We note that a similar law governs in this region the variation of the correction to the thermal coefficient of the electron pressure,¹³ whereas the correction to the conductivity varies more slowly than $z^{-1/2}$ [Eq. (16)]. We emphasize that the absolute value of $Q(z, T)$ tends, together with the normal differential thermoelectric power, linearly to zero as $T \rightarrow 0$.

The calculation of the transverse components of the tensors Q_{ik} and σ_{ik} is similar and shows that, apart from the coefficients, they are subject to the same anomalies as the corresponding longitudinal components. On the other hand, the off-diagonal components of the tensors σ_{ik} and β_{ik} are zero, as can be easily seen from (9).

A similar picture was observed in numerous experiments.^{3-6, 8} Thus, even in the first experiments of Egorov *et al.*³ on $\text{Li}_{1-x}\text{Mg}_x$ alloys, $Q(z)/Q_0$ was a monotonic function at room temperature, while at nitrogen temperatures a pronounced peak appeared at $x = 0.2$, increasing rapidly and becoming somewhat narrower when the temperature was lowered to 4 K. Further lowering of the temperature had no effect whatever on the relative differential thermoelectric power, in full agreement with the proposed theory.

In the experiments of Egorov *et al.*⁴ on $\text{Bi}_{0.9}\text{Sb}_{0.1} + 10^{-4}$ at. % Te, uniaxial deformation resulted in a topological transition connected with the spillover of electrons from two Fermi ellipsoids to a third. Measurement of the differential thermoelectric power at helium temperatures has shown that the peak near the transition point is somewhat asymmetric with a width on the order of several meV, i.e., it cannot be attributed to temperature-induced smearing.

A similar transition was investigated by Gaïdukov *et al.*⁶ by elastically stretching a bismuth whisker. A characteristic plot with a highly asymmetric peak of width ≈ 5 meV was obtained for the thermoelectric power at $T = 5.5$ K; this can likewise be attributed only to impurity smearing.

Brandt *et al.*¹⁴ tracked the evolution, with temperature, of $Q(z)$ for topological transitions in doped $\text{Bi}_{1-x}\text{Sb}_x$ al-

loys, and their results agreed qualitatively with the plot of Fig. 5. In particular, they observed the linear temperature shift of the thermoelectric-power maximum discussed above.

We did not take into account at all in our model effects connected with electron-phonon interactions, although they are undoubtedly quite substantial at sufficiently high temperatures. In the low-temperature region, however, which is of greatest interest from the experimental point of view, the phonons freeze out and these effects can be neglected.

We note that according to the results of Kaganov and Moebius⁷ allowance for the Fermi-liquid interaction does not smear out the Lifshitz topological transition, and only renormalizes the singular parts of the thermodynamic characteristics.

In conclusion, we are deeply grateful to A. A. Abrikosov for suggesting the topic and for constant interest in the work, and thank R. O. Zaitsev for helpful advice, and Yu. P. Gaïdukov, V. S. Egorov, M. Yu. Lavrenyuk, and N. Ya. Minin for a discussion of the experimental results.

¹I. M. Lifshitz, Zh. Eksp. Theor. Fiz. **38**, 1569 (1960) [Sov. Phys. JETP **11**, 1130 (1960)].

²V. G. Vaks, A. V. Trefilov, and S. V. Fomichev, *ibid.* **80**, 1613 (1981) [**53**, 830 (1981)].

³V. S. Egorov and A. N. Fedorovo, *ibid.* **85**, 1647 (1983) [**58**, 959 (1983)]; Pis'ma Zh. Eksp. Teor. fiz. **35**, 375 (1982) [JETP Lett. **35**, 462 (1982)].

⁴V. S. Egorov, N. Yu. Lavrenyuk, N. Ya. Minina, and A. M. Savin, Pis'ma Zh. Eksp. Teor. Fiz. **40**, 25 (1984) [JETP Lett. **40**, 750 (1984)].

⁵S. V. Varyukhin and V. S. Egorov, *ibid.* **39**, 510 (1984) [**39**, 621 (1984)].

⁶Yu. P. Gaïdukov, N. P. Danilova, and E. V. Nikiforenko, *ibid.* **39**, 522 (1984) [**39**, 637 (1984)].

⁷M. I. Kaganov and A. Moebius, Zh. Eksp. Teor. Fiz. **86**, 691 (1984) [Sov. Phys. JETP **59**, 405 (1984)].

⁸N. V. Zavaritskii and N. M. Suslov, *ibid.* **87**, 2152 (1984) [**60**, 1243 (1984)].

⁹D. R. Overcash, T. Davis, J. W. Cook, Jr., and M. J. Skove, Phys. Rev. Lett. **46**, 287 (1981).

¹⁰A. A. Abrikosov, L. P. Gor'kov, and I. E. Dzyaloshinskii, Quantum Field-Theoretical Methods in Statistical Physics, Pergamon, 1965, Chap. VII.

¹¹K. Kubo, J. Phys. Soc. Japan **12**, 570 (1957); R. Kubo, M. Yokota, and S. Nakajima, *ibid.* **12**, 1203 (1957).

¹²A. A. Abrikosov, J. Low Temp. Phys. **10**, 3 (1973).

¹³M. A. Krivoglaz and Tiu-Hao, Fiz. Met. Metalloved. **21**, 817 (1966).

¹⁴N. B. Brandt, V. S. Egorov, M. Yu. Lavrenyuk, N. Ya. Minina, and A. M. Savin, Zh. Eksp. Teor. Fiz. **89**, 2257 (1985) [Sov. Phys. JETP **62**, No. 6 (1985)].

Translated by J. G. Adashko